Revisiting the Spread Spectrum Sliding Correlator: Why Filtering Matters

Ryan J. Pirkl, *Student Member, IEEE,* and Gregory D. Durgin, *Senior Member, IEEE*

***Abstract*—A wireless channel sounder based upon the conventional spread spectrum sliding correlator implementation uses *unfiltered* pseudo-random noise (PN) at both the transmitter and receiver to generate a time-dilated copy of the channel's impulse response. However, in addition to this desired impulse response, the sliding correlator also produces a noise-like, wideband distortion signal that decreases the measurement system's dynamic range. Careful selection of the sliding correlator's low-pass filter can significantly reduce this distortion, but no amount of filtering will remove it completely. In contrast, using *filtered* PNs at both the transmitter and receiver enables one to remove this distortion in entirety and realize a measurement system whose dynamic range closely approximates the theoretical ideal for spread spectrum systems.**

***Index Terms*—Swept time-delay, sliding correlator, spread spectrum technology, impulse response measurements.**

I. Introduction

The utility of the spread spectrum sliding correlator stems from its PN-based *time-dilated autocorrelation*, which packs a wideband probing signal into a relatively narrowband output. This bandwidth compression combined with the time-dilated autocorrelation's large dynamic range has made the spread spectrum sliding correlator an extremely popular platform for performing wideband impulse response measurements [1]–[4]. Despite the architecture's success, realizing the large dynamic range enabled by the spread spectrum sliding correlator's time-dilated PN autocorrelation has long been hindered by the presence of an in-band, noise-like distortion signal. This distortion can severely diminish the output signal's dynamic range and necessitates exhaustive numerical simulations for complete characterization [5], [6].

For most practical applications, however, an impulse response measurement system based upon the spread spectrum sliding correlator will use PNs that have been low-pass filtered, whether deliberately, as illustrated in Fig. 1, or incidentally due to system bandwidth limitations. By using filtered PNs in concert with a judiciously chosen slide factor, one can eliminate the troublesome distortion signal that has plagued the sliding correlator architecture and realize a probing signal whose dynamic range closely approximates the theoretical ideal. Following a brief review of the conventional sliding correlator implementation, we investigate the impact of using *filtered* PNs and develop a simple design rule that ensures a distortion-free time-dilated impulse response measurement.

Manuscript received October 18, 2008; revised February 18, 2009; accepted April 4, 2009. The associate editor coordinating the review of this paper and approving it for publication was A. Molisch.

This work was supported by a National Science Foundation Graduate Research Fellowship.

The authors are with the Propagation Group at the Georgia Institute of Technology (http://www.propagation.gatech.edu).

Digital Object Identifier 10.1109/TWC.2009.081388

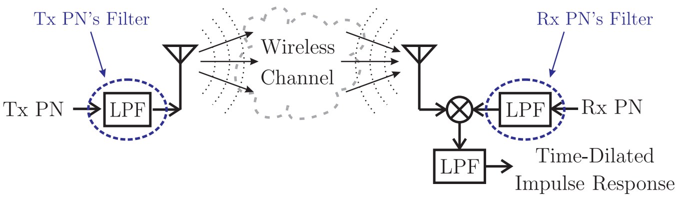

Fig. 1. A complex-baseband diagram of the spread spectrum sliding correlator-based wireless channel sounder highlighting the PNs' low-pass filters that enable a distortion-free time-dilated impulse response. The spread spectrum sliding correlator's time-dilated PN autocorrelation is the probing signal used to measure the complex-baseband wireless channel's impulse response.

II. Pseudo-Random Noise

Pseudo-random noise (PN), denoted $x(t)$, may be derived from a maximal length pseudo-random binary sequence, $a_i \in \{0, 1\}$ [7]. The sequence a_i is periodic such that $a_{i+L} = a_i$, and $x(t)$ is a biphase, unit amplitude analog representation of a_i with a spectrum, $X(f)$, given by [6]

$$X(f) = \frac{1}{L}\sum_{k\in\mathbb{Z}} \operatorname{sinc}\left(\frac{k}{L}\right)\delta\left(f-\frac{f_c k}{L}\right)e^{j\frac{k\pi}{L}} \times \sum_{i=1}^{L}\left[(2a_i-1)e^{-j\frac{k2\pi}{L}i}\right] \quad (1)$$

where $\mathbb{Z}$ is the set of all real integers, f_c is the chip rate, $\delta(\xi)$ is the Dirac delta function, and $\operatorname{sinc}(x) = \frac{\sin(\pi x)}{\pi x}$.

III. Sliding Correlation: Unfiltered PNs

Consider the sliding correlation of two *unfiltered* PNs, $x(t)$ and $x'(t)$, with chip rates, f_c and f'_c, respectively, derived from a maximal length pseudo-random sequence, a_i, of length L. The chip rates are related by the *slide factor*, γ, according to [2]

$$f'_c = f_c\frac{\gamma-1}{\gamma} \quad (2)$$

where $\gamma > 1$ such that $f_c > f'_c$. In the time-domain, the sliding correlator multiplies and then subsequently low-pass filters the two PNs. Thereby, the time-domain output of the sliding correlator is given by

$$y(t) = h_c(t) \otimes [x(t)x'(t)] \quad (3)$$

where $\otimes$ denotes convolution and $h_c(t)$ is the impulse response of the sliding correlator's low-pass filter. It is elucidating to examine the sliding correlator's output in the frequency domain. Denoting $Y(f)$ and $H_c(f)$ as the Fourier transforms of $y(t)$ and $h_c(t)$, respectively, Eq. (3) becomes

$$Y(f) = H_c(f)[X(f) \otimes X'(f)] \quad (4)$$

Carrying out the convolution in (4) yields [6]

$$X(f) \otimes X'(f) = Q_c(f) + Q_d(f) \tag{5}$$

where $Q_c(f)$ is the spectrum for the desired time-dilated autocorrelation as given by

$$Q_c(f) = \frac{1}{L^2} \sum_{k\in\mathbb{Z}} \left\{ \delta\left(f - \frac{f_c k}{\gamma L} \right) \mathrm{sinc}^2\left(\frac{k}{L} \right) \times \sum_{i=1}^{L} \sum_{i'=1}^{L} \left[(2a_i - 1)(2a_{i'} - 1) e^{-j\frac{\pi}{L}k(i-i')} \right] \right\} \tag{6}$$

and $Q_d(f)$ is the spectrum for the unwanted noise or distortion as given by

$$Q_d(f) = \frac{1}{L^2} \sum_{\substack{k,k'\in\mathbb{Z} \\ k'\neq -k}} \left\{ \delta\left(f - \frac{f_c}{L}\left[k + k'\left(\frac{\gamma-1}{\gamma} \right) \right] \right) \times \mathrm{sinc}\left(\frac{k}{L} \right) \mathrm{sinc}\left(\frac{k'}{L} \right) e^{-j\frac{\pi}{L}(k+k')} \times \sum_{i=1}^{L} \sum_{i'=1}^{L} \left[(2a_i - 1)(2a_{i'} - 1) e^{-j\frac{\pi}{L}(ki+k'i')} \right] \right\} \tag{7}$$

In Eq. (7), primed and unprimed summation indices correspond to $X'(f)$ and $X(f)$, respectively. Note that the double summation in $Q_d(f)$ excludes indices related by $k' = -k$, which are the indices from the convolution of $X'(f)$ and $X(f)$ in (5) that correspond to the time-dilated autocorrelation, $Q_c(f)$. Thus, $Q_d(f)$, contains the leftover terms from $X(f) \otimes X'(f)$ that do not correspond to $Q_c(f)$.

Combining (4) and (5) leads to

$$Y(f) = H_c(f)Q_c(f) + H_c(f)Q_d(f) \tag{8}$$

Ideally, we would have $Y(f) = H_c(f)Q_c(f)$ whereby the distortion spectrum, $Q_d(f)$, is completely removed from the sliding correlator's output signal. However, as illustrated by Fig. 2(a), the problem with using unfiltered PNs in the sliding correlator is that $Q_c(f)$ and $Q_d(f)$ will *always* overlap in the frequency domain. Thereby, no choice of the low-pass filter, $H_c(f)$, will completely remove the sliding correlator's distortion spectrum, $Q_d(f)$. Increasing the slide factor will reduce the contribution of $Q_d(f)$ but will never completely eliminate it [6], [8]. The end result is a realized dynamic range well below the theoretical ideal of $20\log_{10}(L)$ dB [3], [5], [6].

IV. Sliding Correlation: Filtered PNs

Fortunately, for many practical applications, the PN will be low-pass filtered to restrict the signal's bandwidth. Let us consider the spectrum of a PN with chip rate, f_c, that has been filtered by an ideal low-pass filter, $H(f)$, with a cut-off frequency at βf_c:

$$H(f) = \begin{cases} 1 & \text{for} \quad |f| \leq \beta f_c \\ 0 & \text{for} \quad |f| > \beta f_c \end{cases} \tag{9}$$

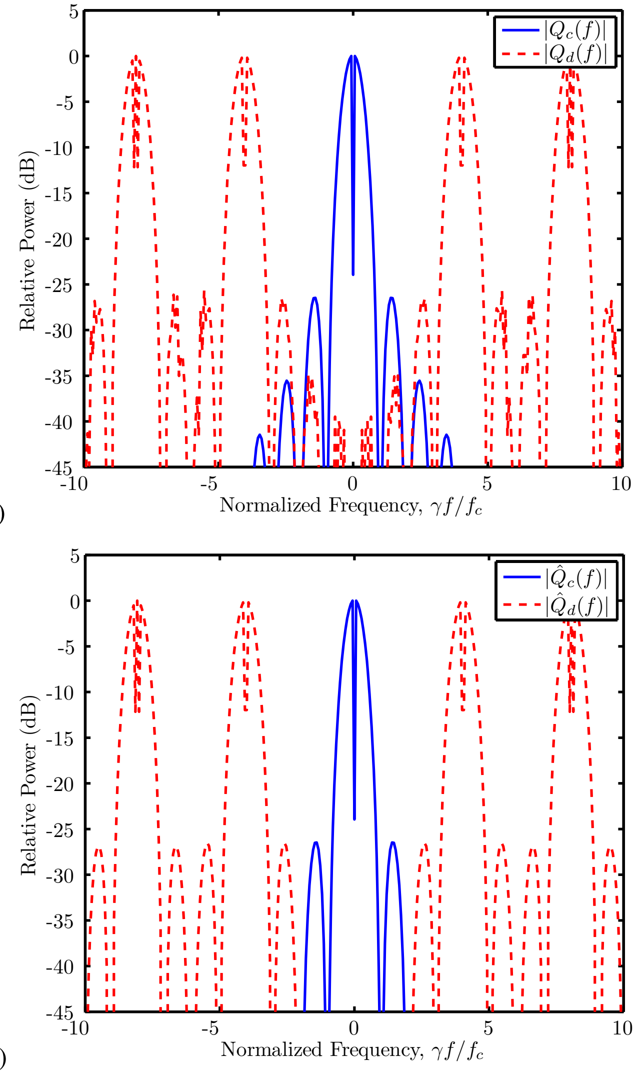

Fig. 2. Envelopes of the time-dilated autocorrelation spectrum and distortion spectrum produced by a sliding correlator using PNs of length $L = 15$ and a slide factor of $\gamma = 4L + 1$: (a) *unfiltered* PNs and (b) *filtered* PNs using filters characterized by $\beta = \beta' = 2$.

Using (9), the filtered PN's spectrum, denoted $\hat{X}(f)$, may be expressed as

$$\hat{X}(f) = X(f)H(f) \tag{10}$$

Equivalently, $\hat{X}(f)$ corresponds to the original spectrum defined in (1) whereby the infinite summation is truncated such that k is restricted to

$$|k| \leq k_{\max} = \lfloor(\beta L)\rfloor \tag{11}$$

In Eq. (11), $\lfloor(\cdot)\rfloor$ denotes the *floor* function.

Similarly, filtering the PN spectrum $X'(f)$ (with chip rate f'_c) by an ideal low-pass filter, $H'(f)$, defined as

$$H'(f) = \begin{cases} 1 & \text{for} \quad |f| \leq \beta' f'_c \\ 0 & \text{for} \quad |f| > \beta' f'_c \end{cases} \tag{12}$$

produces a filtered PN spectrum, $\hat{X}'(f)$ given by

$$\hat{X}'(f) = X'(f)H'(f) \tag{13}$$

This is equivalent to truncating $X'(f)$'s infinite summation with respect to the summation index k' such that

$$|k'| \leq k'_{\max} = \lfloor(\beta' L)\rfloor \tag{14}$$

A. Bounds on Time-Dilated Autocorrelation Spectrum

With these bounds on the summation indices, k and k', for the filtered PN spectra, $\hat{X}(f)$ and $\hat{X}'(f)$, respectively, consider the filtered PNs' time-dilated autocorrelation spectrum, $\hat{Q}_c(f)$. By inspection of the *unfiltered* PNs' time-dilated autocorrelation defined in Eq. (6), it may be found that the maximum frequency at which the *filtered* PNs' time-dilated autocorrelation is nonzero is given by

$$f_{\max}^{\hat{Q}_c} = \max\left\{\frac{f_c k}{\gamma L}\right\} \tag{15}$$

whereby

$$\hat{Q}_c(f) = 0 \text{ for } |f| > f_{\max}^{\hat{Q}_c} \tag{16}$$

In (15), $\max\{(\cdot)\}$ denotes the maximum value of the set $\{(\cdot)\}$. Recalling that $\hat{Q}_c(f)$ corresponds to $\hat{X}(f) \otimes \hat{X}'(f)$ for the case that $k' = -k$, we find that $f_{\max}^{\hat{Q}_c}$ is maximized by setting k to the minimum of $k_{\max}$ and $k'_{\max}$. With the aid of Eqs. (11) and (14), (15) becomes

$$f_{\max}^{\hat{Q}_c} = \frac{f_c}{\gamma L}\lfloor(\min\{\beta, \beta'\}L)\rfloor \tag{17}$$

In (17), $\min\{(\cdot)\}$ indicates the minimum value of the set $\{(\cdot)\}$. Thereby, $f_{\max}^{\hat{Q}_c}$ specifies an upper bound on the nonzero spectral content of $\hat{Q}_c(f)$.

B. Bounds on Distortion Spectrum

For the filtered PNs' distortion spectrum, denoted $\hat{Q}_d(f)$, we are interested in identifying the smallest positive frequency at which $\hat{Q}_d(f)$ is nonzero. Therefore, we seek to minimize the argument of the Dirac delta function in Eq. (7):

$$f_{\min}^{\hat{Q}_d} = \min\left\{\frac{f_c}{L}\left[k + k'\left(\frac{\gamma - 1}{\gamma}\right)\right]\right\} \tag{18}$$

whereby

$$\hat{Q}_d(f) = 0 \text{ for } |f| < f_{\min}^{\hat{Q}_d} \tag{19}$$

Determination of $f_{\min}^{\hat{Q}_d}$ is considerably more involved than $f_{\max}^{\hat{Q}_c}$, and details of the derivation may be found in the Appendix. The final result is

$$f_{\min}^{\hat{Q}_d} = \frac{f_c}{L}\left[1 - \frac{1}{\gamma}\lfloor(\min\{\beta', \beta + 1/L\}L)\rfloor\right] \tag{20}$$

with the added constraint that $\gamma > \lfloor(\min\{\beta', \beta + 1/L\}L)\rfloor$ so as to ensure that $f_{\min}^{\hat{Q}_d} > 0$.

C. Condition for Orthogonal Spectra

Provided that $f_{\min}^{\hat{Q}_d} > f_{\max}^{\hat{Q}_c}$, $\hat{Q}_c(f)$ and $\hat{Q}_d(f)$ will have no overlap in their spectra. Thereby, with an appropriate choice of low-pass filter, one may *completely* remove the sliding correlator's distortion spectrum, $\hat{Q}_d(f)$ without altering the time-dilated autocorrelation spectrum, $\hat{Q}_c(f)$. The condition for the slide factor that ensures orthogonality in the spectra is

$$\gamma > \lfloor\min\{\beta, \beta'\}L\rfloor + \lfloor\min\{\beta', \beta + 1/L\}L\rfloor \tag{21}$$

For the case of $\beta = \beta'$, dividing Eq. (21) by L leads to the following convenient design equation:

$$\frac{\gamma}{L} > 2\beta \tag{22}$$

Figure 2(b) presents the filtered PNs' time-dilated autocorrelation spectrum, $\hat{Q}_c(f)$, and distortion spectrum, $\hat{Q}_d(f)$, for the case of $L = 15$, $\beta = \beta' = 2$, and $\gamma = 4L + 1$. Note that, aside from using filtered PNs, this corresponds directly to the spectra presented in Fig. 2(a). In contrast to the unfiltered PNs, the filtered PNs' distortion spectrum is clearly orthogonal to the time-dilated autocorrelation spectrum. This enables removal of $\hat{Q}_d(f)$ with appropriate selection of the low-pass filter, $H_c(f)$.

D. Distortion-Free Time-Dilated Autocorrelation

Provided that Eq. (21) is satisfied, one may completely remove $\hat{Q}_d(f)$ without alteration to $\hat{Q}_c(f)$ by using an ideal rectangular low-pass filter whose pass-band extends to $f_{\max}^{\hat{Q}_c}$ and whose stop-band begins at $f_{\min}^{\hat{Q}_d}$. Thereby, we require the sliding correlator's low-pass filter $H_c(f)$ to have the following properties:

$$H_c(f) = \begin{cases} 1 & \text{for} \quad |f| \leq f_{\max}^{\hat{Q}_c} \\ 0 & \text{for} \quad |f| \geq f_{\min}^{\hat{Q}_d} \end{cases} \tag{23}$$

Replacing $Q_c(f)$ and $Q_d(f)$ in Eq. (8) with $\hat{Q}_c(f)$ and $\hat{Q}_c(f)$, respectively, and using the frequency bounds on the spectra given in (16) and (19) in concert with an $H_c(f)$ satisfying (23), one finds that the sliding correlator's output is exactly $\hat{Q}_c(f)$:

$$Y(f) = H_c(f)[\hat{Q}_d(f) + \hat{Q}_d(f)] = \hat{Q}_c(f) \tag{24}$$

The sliding correlator's distortion-free time-dilated autocorrelation will have a dynamic range, D_R, that closely approximates the dynamic range of a PN's autocorrelation:

$$D_R \approx D_{R,\text{ideal}} = 20\log_{10} L \text{ (dB)} \tag{25}$$

The approximation in Eq. (25) arises due to $\hat{Q}_c(f)$'s finite bandwidth, which results from the necessary filtering operations. The PN's low-pass filters $H(f)$ and $H'(f)$, as well as the sliding correlator's filter, $H_c(f)$, remove high-frequency content from $\hat{Q}_c(f)$ and smooth the otherwise sharp, triangular pulse of the PN's autocorrelation. This leads to a reduced peak amplitude as well as an increase in the pulse's full-width half-maximum. The resulting reduction in dynamic range and temporal resolution will depend on the specific choice of L, β, and β', but will generally be around one or two dB.

V. Physically Realizable Filters

Although the preceding analysis assumed ideal rectangular low-pass filters, the dynamic range of the sliding correlator will also improve if the PNs are filtered with physically realizable low-pass filters. To demonstrate this, we simulated

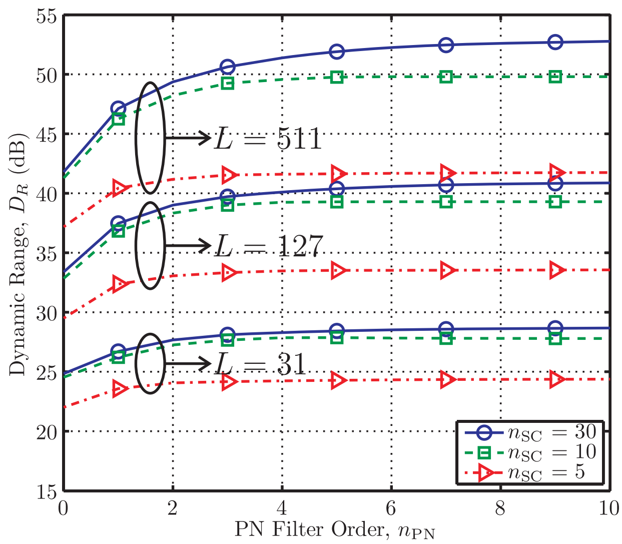

Fig. 3. A comparison of the dynamic range of the spread spectrum sliding correlator for various PN filter orders, n_{PN}, sliding correlator filter orders, n_{SC}, and PN lengths, L. The dynamic range at $n_{\mathrm{PN}} = 0$ corresponds to the performance of a spread spectrum sliding correlator using *unfiltered* PNs.

using Butterworth filters for both the PNs' low-pass filters, $H(f)$ and $H'(f)$, and the sliding correlator's low-pass filter, $H_c(f)$. The PNs were filtered by Butterworth low-pass filters of order n_{PN} with a -3 dB cut-off corresponding to the PNs' chip rates, f_c and f_c', respectively ($\beta = \beta' = 1$). The resulting filtered PNs were multiplied and subsequently filtered by the sliding correlator's low-pass filter, $H_c(f)$, which was realized by a Butterworth low-pass filter of order n_{SC} with a -3 dB cut-off at f_c/γ. The slide factor was set to $\gamma = 2\beta L + 1$, and the sliding correlator's dynamic range was calculated using [6]

$$D_R = 20\log_{10}\left(\frac{\max\left|\mathcal{F}^{-1}\left\{L\hat{Q}_c(f)H_c(f)\right\}\right|}{\max\left|\mathcal{F}^{-1}\left\{L\hat{Q}_d(f)H_c(f)-1\right\}\right|}\right)\ \mathrm{dB} \tag{26}$$

where $\mathcal{F}^{-1}$ denotes the inverse Fourier transform.

Figure 3 presents the dynamic range of the sliding correlator based on filtered PNs for $L = \{31, 127, 511\}$; *unfiltered* PNs corresponding to $n_{\mathrm{PN}} = 0$. As Fig. 3 indicates, unfiltered PNs lead to the worst dynamic range for a given PN length, L, and sliding correlator low-pass filter order, n_{SC}. More so, the improvements afforded by filtering the PNs were considerable for Butterworth filters of reasonably small order (e.g., $n_{\mathrm{PN}} \approx 3$). It should be emphasized that this was achieved with Butterworth filters; filter topologies like the Chebyshev filter, which has a sharper transition from pass-band to stop-band, should provide comparable dynamic range improvements with lower order filters.

VI. Conclusion

By low-pass filtering the PNs and selecting a slide factor that satisfies the inequality presented in Eq. (21), it is possible to *completely* eliminate the distortion signal that has plagued the sliding correlator architecture. This enables the spread spectrum sliding correlator to produce a distortion-free time-dilated autocorrelation with a dynamic range that closely approximates the theoretical ideal.

Appendix

We begin by rewriting (18) as

$$f_{\min}^{\hat{Q}_d} = \frac{f_c}{L}\min\left\{k + k'\frac{\gamma-1}{\gamma}\right\} \tag{27}$$

Enforcing the requirement that $f_{\min}^{\hat{Q}_d} > 0$, we observe that

$$k' > -k\frac{\gamma}{\gamma-1} \tag{28}$$

Recalling that $(\gamma-1)/\gamma \in (0,1)$, inspection of Eq. (27) reveals that $f_{\min}^{\hat{Q}_d}$ can only be minimized for integer k and k' if

$$\mathrm{sgn}(k) = -1 \tag{29}$$

In (29), $\mathrm{sgn}(\cdot)$ indicates the sign of $(\cdot)$. Using (29), (28) may be reexpressed as

$$\frac{k'}{-k} > \frac{\gamma}{\gamma-1} > 1 \tag{30}$$

Consideration of Eq. (30) in the the context of the overarching minimization problem reveals that we require the smallest ratio of $k'/(-k)$ that is greater than $\gamma/(\gamma-1)$. Provided that $k' < \gamma$, this is achieved by

$$k = 1 - k' \text{ for } k' < \gamma \tag{31}$$

where

$$k' = \min\{k'_{\max}, k_{\max} + 1\} \tag{32}$$

For $k' \geq \gamma$, (27) allows for $f_{\min}^{\hat{Q}_d} \leq 0$ such that $\hat{Q}_d(f)$ has no minimum positive frequency component. Thus we require that $k' < \gamma$. Substituting (31) and (32) into (27) yields the final result presented in Eq. (20).

References

[1] N. Benvenuto, "Distortion analysis on measuring the impulse response of a system using a crosscorrelation method," *AT&T Bell Laboratories Techn. J.*, vol. 63, no. 10, pp. 2171–2192, Dec. 1984.

[2] D. C. Cox, "Delay Doppler characteristics of multipath propagation at 910 MHz in a suburban mobile radio environment," *IEEE Trans. Antennas and Propagation*, vol. 20, no. 5, pp. 625–635, Sept. 1972.

[3] W. G. Newhall, T. S. Rappaport, and D. G. Sweeney, "A spread spectrum sliding correlator system for propagation measurements," *RF Design*, pp. 40–54, Apr. 1996.

[4] C. R. Anderson, "Design and implementation of an ultrabroadband millimeter-wavelength vector sliding correlator channel sounder and in-building multipath measurements at 2.5 & 60 GHz," Master's thesis, Virginia Tech, May 2002, online: http://scholar.lib.vt.edu/theses/available/etd-05092002-101656/unrestricted/AndersonThesisETD.pdf.

[5] G. Martin, "Wideband channel sounding dynamic range using a sliding correlator," in *Proc. VTC 2000-Spring Tokyo*, ser. VTC Conf. Proc., vol. 3, May 15-18 2000, pp. 2517–2521.

[6] R. J. Pirkl and G. D. Durgin, "Optimal sliding correlator channel sounder design," *IEEE Trans. Wireless Commun.*, vol. 7, no. 9, pp. 3488–3497, Sept. 2008.

[7] S. W. Golomb, *Shift Register Sequences*, revised ed. Laguna Hills, CA: Agean Park Press, 1982.

[8] J. Talvitie and T. Poutanen, "Self-noise as a factor limiting the dynamic range in impulse response measurements using sliding correlation," in *Proc. IEEE International Symposium on Spread Spectrum Techniques and Applications '94*, 4-6 July 94, pp. 619–623.